Synsint Research Group

Available online at www.synsint.com

Synthesis and Sintering

ISSN 2564-0186 (Print), ISSN 2564-0194 (Online)

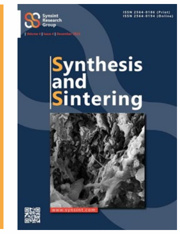

Research article

Neutron shielding performance of polyethylene-7% B and Al-30 wt% B_4C composites fabricated via hot-press sintering

Check for updates

Masomeh Ghayebloo [a], Zeinab Naghsh Nejad [b], Nafiseh Araghian [b], Hamzeh Foratirad [c,*], Amir Movafeghi [b]

[a] *Department of Materials Science and Engineering, University of Bonab, P.O. Box 5551761167, Bonab, Iran*
[b] *Reactor and Nuclear Safety Research School, Nuclear Science and Technology Research Institute (NSTRI), Tehran, Iran*
[c] *Nuclear Fuel Cycle Research School, Nuclear Science and Technology Research Institute (NSTRI), Tehran, Iran*

ABSTRACT

The current research investigates the neutron shielding features of polyethylene-7% B and Al-30 wt% B_4C composites fabricated via hot-press sintering. The practical analysis was conducted via Neutron radiography and Monte Carlo N-Particle (MCNP) simulation. The results illustrated that Al-30 wt% B_4C with 5 mm thickness has equivalent neutron absorption properties with 14 mm thickness of PE-7% B. Composites with higher density and homogenous distribution of B_4C have better neutron shield properties. Al-30 wt% B_4C composite fabricated at 650 °C has a higher neutron absorption property. Experimental and simulation findings confirmed each other at lower thicknesses and Al-30 wt% B_4C has better neutron shielding than PE-7% B. At thicknesses over 1 cm, the cross-sectional area of polyethylene-7% B and Al-30 wt% B_4C composites are near each other. By increasing the thicknesses of composites, the relative total dose reduction and the shield properties of composites are enhanced.

KEYWORDS

Hot-press
Monte Carlo
Neutron radiography
Neutron shielding

OPEN ACCESS

1. Introduction

Recently, the most common material used for dry pools of nuclear fuel equipment is metal casks [1]. The storing ability of the spent nuclear fuel has been increased by using high-density shields. However, these shields must also decrease the neutron radiations [2]. Dual-purpose casks are utilized for both transporting and storing spent nuclear fuel in industries. The cask basket is fabricated from Al-B composites [1]. Also, boron-containing alloys are used in the fabrication of dual-purpose casks [3].

In general, the commercial names of neutron absorption materials are Boraflex, boron-contained stainless steel alloys, and Al-B alloys [4]. These materials are widely used as fuel storage baskets. The main problem with this equipment is controlling the size and distribution of B in the Al-B_4C composites [5–6].

B_4C is one of the ceramic materials that have high strength, low density, thermal stability, and high neutron absorption [7–9]. Boron carbide absorbs neutrons [10–12] due to the high thermal neutron absorption cross-section of ^{10}B [13]. The ^{10}B absorbs thermal neutrons, whereas ^{11}B acts as a neutron reflector [14, 15].

Al-B_4C composites are employed to absorb neutrons and obstacles in front of neutron radiations. These composites are lightweight and highly thermal conductive and are utilized as a basket in nuclear casks [16–21]. Polyethylene-boron composites are used as efficient neutron shields due to the high neutron absorption capacity of boron [22].

* Corresponding author. *E-mail address:* hforatirad@aeoi.org.ir (H. Foratirad)
Received 23 September 2024; Received in revised form 31 October 2024; Accepted 11 November 2024.

https://doi.org/10.53063/synsint.2024.44250

In-practical, Al/B_4C composites will be exposed to irradiate neutrons radiation in (0.25–26)×10^4/cm^2.s [23, 24]. In practice, Al-B_4C composites are used at 250–350 °C temperatures [25–28].

Igwesi et al. reported thermal neutron macroscopic cross-sections for both pure polythene and borated polythene at various thicknesses. They computed neutron macroscopic cross-sections from the MCNP simulations. The result showed that these materials are excellent for neutron shielding [29].

Zhang et al. employed B_4C/Al composites with a thickness of 5 mm, in comparison to a 0.5 mm-thick Cd plate, using the unidirectional neutron beam diffusion method to obtain neutron absorption. The results illustrated that a 5 mm-thick Al-30 wt% B_4C composite absorbs the same amount of neutrons as a 0.5 mm-thick Cd plate [24].

As mentioned above, Al-B_4C composites are unique products in nuclear industries. In the field of neutron radiation protection, proper protection should be to decrease the rate of the neutron and thus attenuate it. Since the neutron shielding mechanism is the goal of this study, the neutron transmission of polyethylene-7% B and Al-30 wt% B_4C composite as neutron absorbers is investigated. We compared neutron absorption properties via Neutron radiography and MCNP simulation.

2. Methods and experiments

2.1. Al-30 wt% B_4C fabrication

2.1.1. Milling

First, B_4C (99.99%, 45 µm, Russia) and Al (99.99%, 20 µm, Fluka, Belgium) were blended for preparation of Al-30 wt% B_4C composite. For this purpose, raw materials were milled in planetary ball milling (model: Fritsch, Pulverisette 5) under an Ar atmosphere, at 190 rpm with a tungsten carbide ball-to-powder ratio of 2:1 for 4 h using 2 wt% of absolute ethyl alcohol (99.7 vol%).

The milling process was done at 190 rpm with a tungsten carbide ball-to-powder ratio of 2:1 for 4 hours and 2 wt% absolute ethyl alcohol (99.7 vol%) media.

2.1.2. Forming and sintering

To fabricate the hot pressed samples, 6 g of the mixed raw material was placed in a graphite die with a 10 mm diameter and sintered at temperatures of 550, 600, and 650 °C using an HP machine (Shenyang Weitai Science & Technology Development Co., Ltd.). During sintering, the temperature was raised from room temperature to 500 °C at a rate of 5 °C/min. The temperature was then increased at a rate of 5 °C/min to 550, 600, and 650 °C, while the external pressure was gradually raised to 50 MPa. At each final temperature (550, 600, and 650 °C), the pressure was maintained at 50 MPa for 1 hour under a vacuum of 5×10^{-2} Pa. In the end, the applied pressure was released, and the composites were slowly cooled. Table 1 shows the features of composites.

2.2. Borated polyethylene (PE-7% B)

As a protective shield, borated polyethylene (PE-7% B) is utilized for neutron absorption [22]. In the present research, it was fabricated in step wedge for analysis with prepared composites.

2.3. Characterization

2.3.1. Physical characteristics

Bulk density and the thickness of Al-30 wt% B_4C composites were obtained by Archimedes' technique based on C 373–88 of ASTM standard [30].

2.3.2. Neutron radiography analysis

The composites were analyzed using Neutron radiography (NR) at the neutron digital imaging facility of the Tehran Research Reactor (Fig. 1). Results were processed by ImageJ software version 2.16.0. Due to the small size of the specimens and to prevent the adverse effects of scattered neutrons on the neutron transmission measurement, the surround of the neutron detector behind each specimen or step wedge was covered with a sheet of cadmium.

2.3.3. Monte Carlo simulation

Simulation calculations have been done using MCNPX code version 2.7. The code is versatile radiation transport software that employs the Monte Carlo technique to track different particle types across a broad energy spectrum. By determining the exact structure of the radiographic beam tube, the samples, and also the neutron flux, and by using the appropriate tally cards, outputs have been obtained. In these simulations, the samples are considered as bulk [31]. To simulate the neutron transmission value, a wedge made of polyethylene-7% boron and samples made of Al-30 wt% B_4C composite were modeled in the Monte Carlo N-Particle (MCNP) transport program code. Then, the neutron flux was calculated before the incident with the samples or each step of the polyethylene wedge and after transmission.

3. Results and discussion

Neutron absorption characteristics of (PE-7% B) and Al-30 wt% B_4C samples were studied through experimental NR and MCNP simulation.

Fig. 1. Arrangement of Neutron radiography test.
Left side: Al-30 wt% B_4C; right side: PE-7% B.

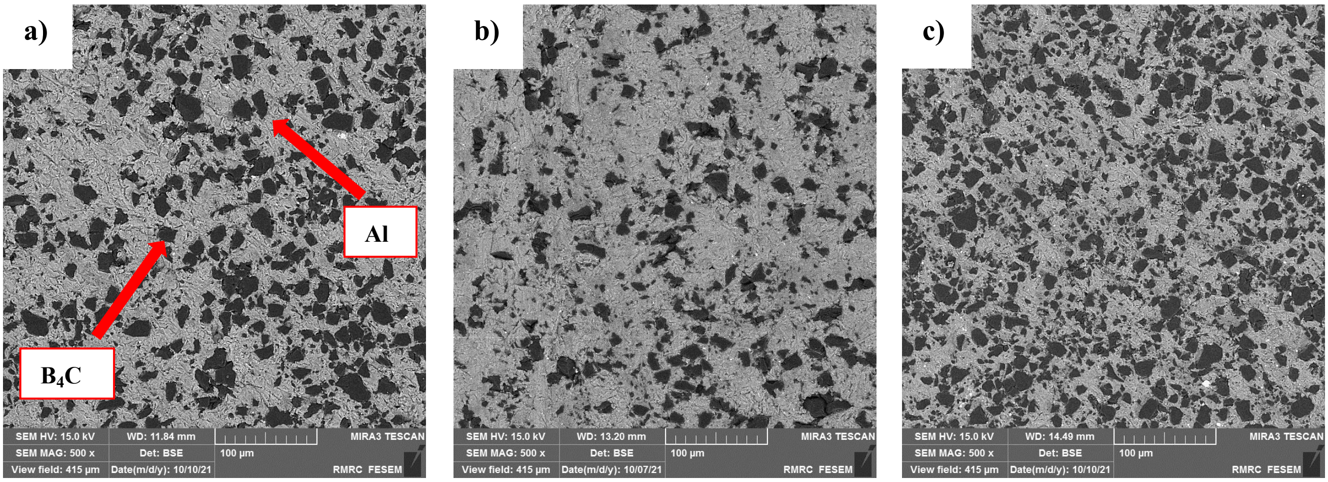

Fig. 2. The FESEM images from the polished surfaces of composites at: a) 550 °C, b) 600 °C, and c) 650 °C.

3.1. Experimental results

In the experimental results, the samples with higher homogenous distribution of B_4C particles and density have a distinguish neutron protection feature. For example, composite fabricated at 650 °C has the highest neutron attenuation features. As can be seen from Fig. 2, the sample fabricated at 650 °C has homogeneous distribution of B_4C.

In Zhang et al. report, composites containing over 30 wt% of B_4C (fabricated by hot-press method at 630 °C) in comparison with cadmium, showed better attenuation neutron properties [24]. The bulk density and thickness of Al-30 wt% B_4C samples are shown in Table 1.

Neutron radiography (NR) image of samples was indicated in Fig. 3. The mean gray values corresponding to the thickness of the composites are presented in Fig. 4. The results illustrated the Al-30 wt% B_4C with 5 mm thickness has equivalent neutron absorption properties with 14 mm thickness of PE-7% B.

3.2. Simulation results

To compare the neutron transmission value of wedge polyethylene-7% B and Al-30 wt% B_4C composites were modeled in MCNP code. The results of this calculation are given in Fig. 5. As observed in Fig. 5, a polyethylene sample with a thickness of 0.2 cm transmitted about 90% of the neutron beam, while the Al-30 wt% B_4C composite sample of the same thickness transmitted about 70% of the neutron beam.

Table 1. Thickness and bulk density of Al-30 wt% B_4C samples.

Sample name	Thickness (mm)	Bulk density (g/cm^3)
1	2.5	2.2919
2	4.5	2.4844
3	5	2.2919
4	7	2.5011
5	8	2.4844

The sample with 0.2 cm thickness of polyethylene and Al-30 wt% B_4C composite transmitted about 90% and 70% of the neutron beams (Fig. 5). It indicated better neutron absorption by the Al-30 wt% B_4C composite sample. This process of neutron absorption can also be well observed in the 0.4 cm thickness of samples. As the thickness of the samples increased, the neutron beam transmission or absorption in Al-30 wt% B_4C composite samples gradually approached that of polyethylene-7% B.

The density, shape, cross-section, and geometric dimensions of the Al-30wt% B_4C composite specimens differed from those of the polyethylene wedge. So, to better understand the neutron absorption performance of Al-30 wt% B_4C composite, an Al-30 wt% B_4C wedge with the same dimensions and

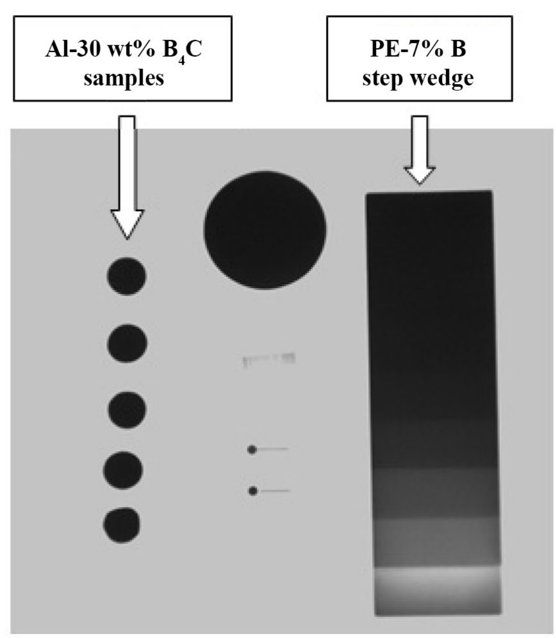

Fig. 3. The Neutron radiography of Al-30 wt% B_4C and PE-7% B.

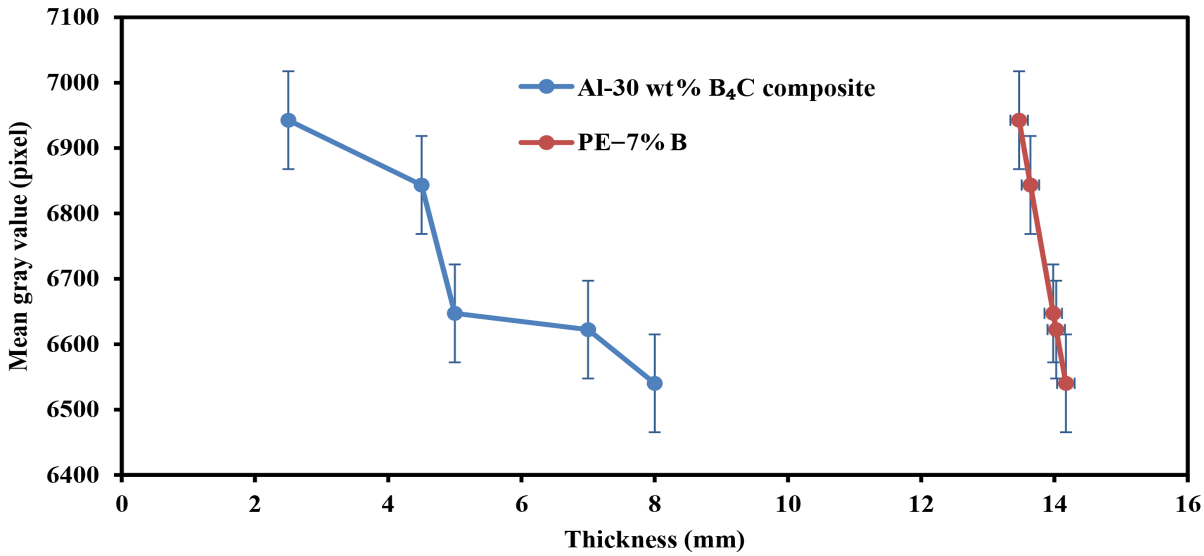

Fig. 4. The mean gray value of Al-30 wt% B_4C and PE-7% B wedges according to thicknesses (calculation error <4%).

appearance as a polyethylene wedge was modeled. The neutron transmittance and macroscopic cross-section were measured versus thickness by using MCNP calculations. It should be noted that the density of the Al-30 wt% B_4C wedge was considered equal to the density of one of the samples (sample number 4: 2.5011 g/cm^3). The results of this calculation have been shown in Fig. 6. Also, according to Fig. 6, it can be observed the high absorption of neutrons at low thicknesses of Al-30 wt% B_4C composite. Also, the Al-30 wt% B_4C composite has a high absorption of neutrons at low thicknesses (Fig. 6). The absorption of neutrons ability decreases with increasing the thickness of the Al-30 wt% B_4C composite. At 0.8 cm thickness, the neutron transmittance of both samples is equal, and with increasing the thickness, the performance of the two samples is close to each other.

As can observed from Fig. 7, in collisions with neutrons at less

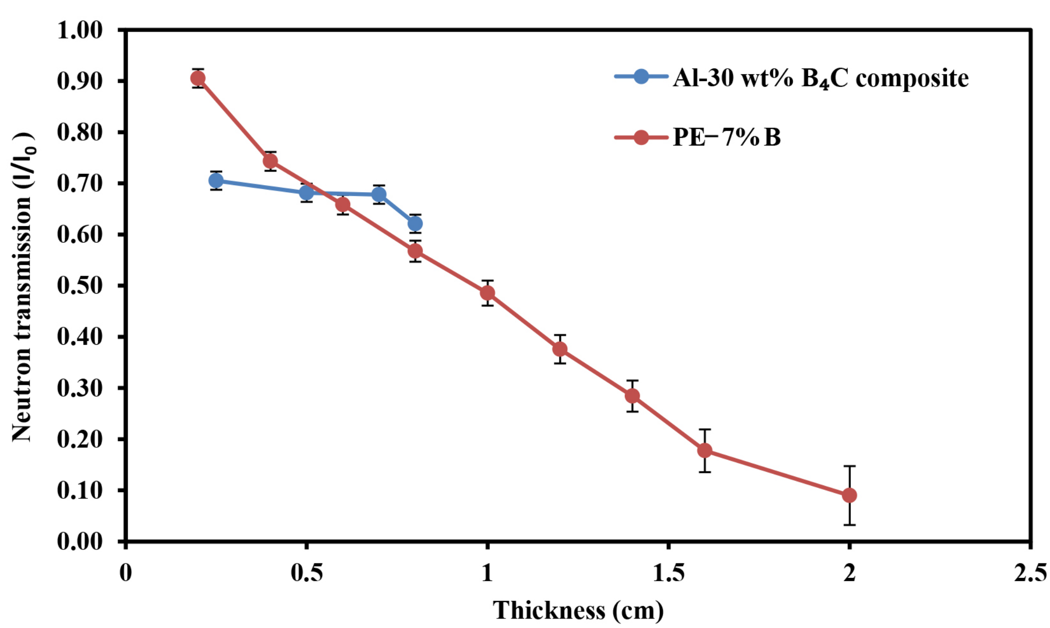

Fig. 5. The results of the simulation of the neutron transmission of Al-30 wt% B_4C samples and PE-7% B step wedge (calculation error <0.5%).

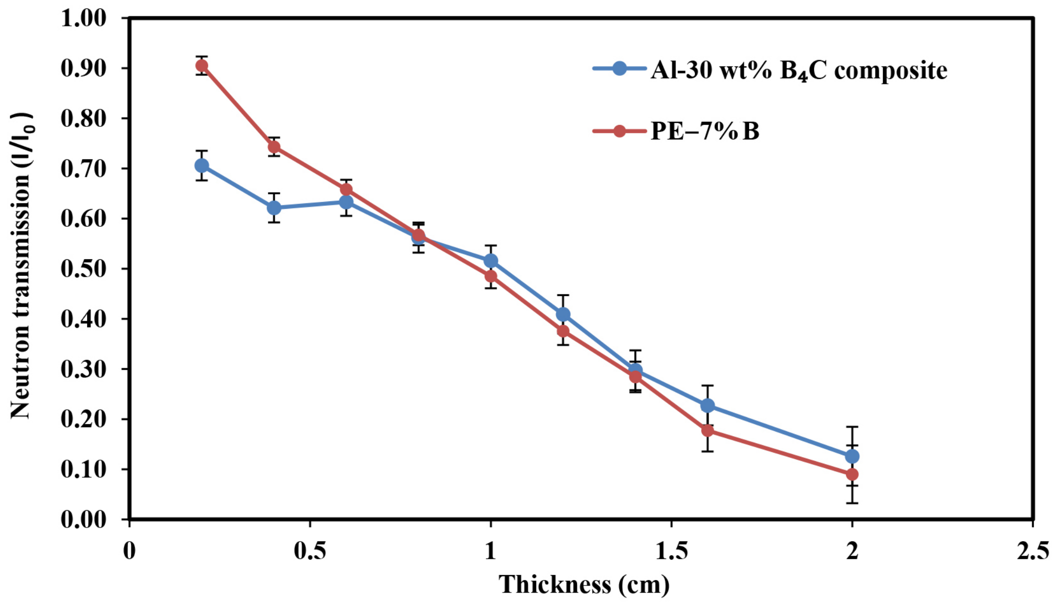

Fig. 6. The result of the simulation of comparison of the neutron transmission of the polyethylene 7% B wedge and Al-30 wt% B_4C composite wedge.

than 0.5 cm of thickness, the shield features of Al-30 wt% B_4C samples are higher than PE-7% B. Additionally, the composite reduces the neutron dose by approximately 20 to 25%, while polyethylene reduces it by about 10% at the same lower thicknesses. To follow, it can be observed clearly in Fig. 5, that with the increasing thickness of composites, the shield properties of Al-30 wt% B_4C and polyethylene are similar. When the thicknesses of composites increased, the relative total dose reduction of the samples enhanced (Fig. 7), and the shield properties of composites enhanced.

Fig. 8 shows the cross-sectional changes with increasing thickness. As the thickness increases, the cross-sectional area decreases. Materials with a high neutron absorption cross-section are suitable for absorbing thermal neutrons. At low thicknesses, the cross-sectional area of Al-30 wt% B_4C composite for neutron absorption is much higher than polyethylene (Fig. 8). As the thickness increases, the cross-sectional area decreases. At thicknesses over 1 cm, the cross-sectional areas of both materials are very similar and close to each other.

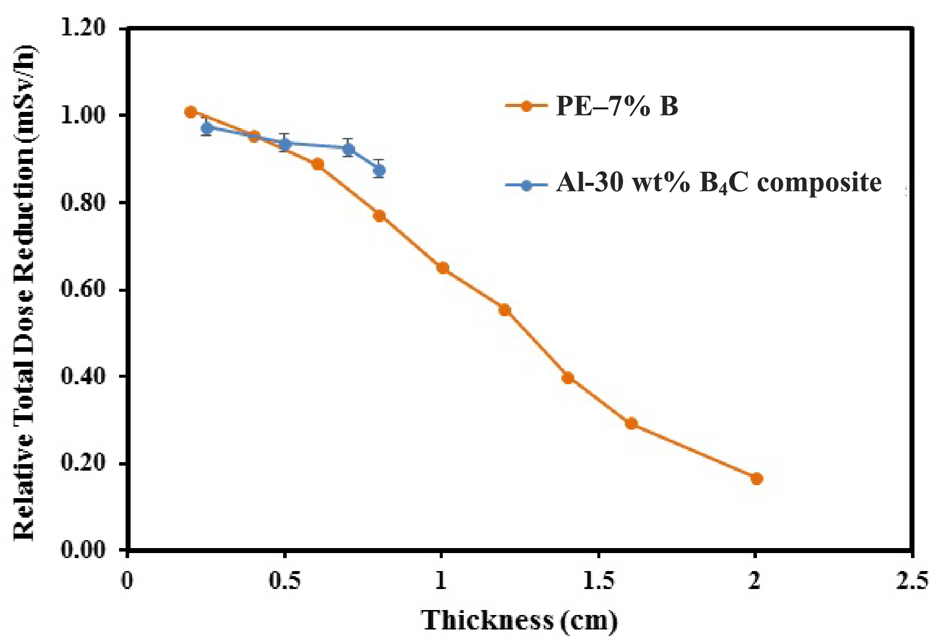

Fig. 7. Relative total dose reduction as a function of the thickness of polyethylene-7% B and Al-30% B_4C.

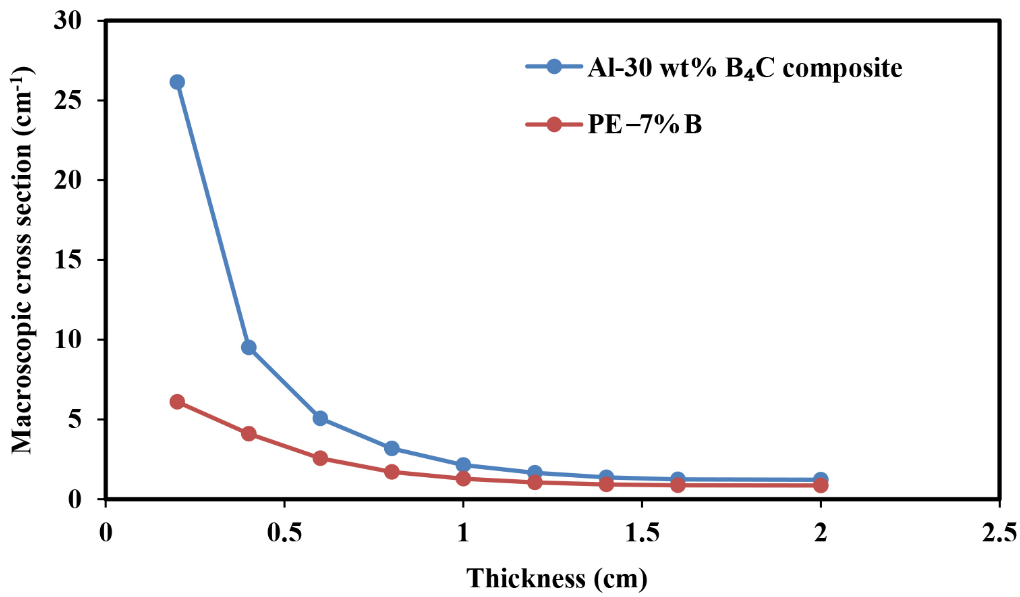

Fig. 8. Relative comparison of the macroscopic cross-section of polyethylene-7% B and Al-30 wt% B_4C composite wedges.

4. Conclusions

- At equal neutron absorption intensities, the Al-30 wt% B_4C composite fabricated in this report is equal to half of the thickness of the polyethylene-7% B composite
- Experimental and simulation results confirm that, at lower thicknesses, the Al-30 wt% B_4C composite offers superior neutron shielding performance compared to PE-7% B.
- Al-30 wt% B_4C composite fabricated at 650 °C has higher neutron absorption properties due to the uniform dispersion of B_4C grains and its higher density.
- In the lower thicknesses, Al-B_4C composites have better neutron absorption.
- At thicknesses over 1 cm, the cross-sectional areas of both materials are very similar and close to each other.

CRediT authorship contribution statement

Masomeh Ghayebloo: Conceptualization, Data curation, Formal analysis, Investigation, Methodology, Writing – original draft.
Zeinab Naghsh Nejad: Simulation, Conceptualization, Data curation, Formal analysis, Investigation, Methodology, Writing – original draft.
Nafiseh Araghian: Conceptualization, Formal analysis.
Hamzeh Foratirad: Supervision, Writing – review & editing, Project administration.
Amir Movafeghi: Conceptualization, Formal analysis.

Data availability

The data underlying this article will be shared on reasonable request to the corresponding author.

Declaration of competing interest

The authors declare no competing interests.

Funding and acknowledgment

This research received a grant (number: LMO-2-C-MP-9906-02) from funding leading material organization, Nuclear Science and Technology Research Institute (NSTRI).

References

[1] G. Jobson, H. Spilker, D. Methling, Castor® X/32 s—a New Dual-Purpose Cask for the Storage and Transport of Spent Nuclear Fuel, WM'00 Conference, Tucson, AZ. (2000) 39.
[2] Y. Jung, M. Lee, K. Kim, S. Ahn, 10B (n, α) 7Li reaction-induced gas bubble formation in Al–B4C neutron absorber irradiated in spent nuclear fuel pool, J. Nucl. Mater. 533 (2020) 152077. https://doi.org/10.1016/j.jnucmat.2020.152077.
[3] J. Ko, J. Park, I. Jung, G. Lee, C. Baeg, T. Kim, Shielding analysis of dual purpose casks for spent nuclear fuel under normal storage conditions, Nucl. Eng. Technol. 46 (2014) 547–556. https://doi.org/10.5516/NET.08.2013.039.
[4] J.M. Solano, T. Page, T. Hicks, P. Thorne, The use of Neutron-absorbing Materials in ILW and Spent Fuel Packages for Criticality Control, Nuclear Decommissioning Authority: Moor Row, UK. (2012).
[5] M. Ravichandran, A. Manikandan, M. Sundaram Omkumar, Investigations on properties of Al-B4C composites synthesized through powder metallurgy route, Appl. Mech. Mater. 852 (2016) 93–97. https://doi.org/10.4028/www.scientific.net/AMM.852.93.
[6] G. Bonnet, V. Rohr, X.-G. Chen, J.-L. Bernier, R. Chiocca, H. Issard, Use of Alcan's Al-B4C metal matrix composites as neutron absorber material in TN International's transportation and storage casks, Packag., Transp., Storage Secur. Radioact. Mater. 20 (2009) 98–102. https://doi.org/10.1179/174651009X416880.
[7] G. Manohar, K. Pandey, S. Maity, Characterization of Boron Carbide (B4C) particle reinforced aluminium metal matrix composites fabricated by powder metallurgy techniques–A review, Mater. Today Proc. 45 (2021) 6882–6888. https://doi.org/10.1016/j.matpr.2020.12.1087.

[8] M. Paidar, O. Oladimeji Ojo, H. Ezatpour, A. Heidarzadeh, Influence of multi-pass FSP on the microstructure, mechanical properties and tribological characterization of Al/B4C composite fabricated by accumulative roll bonding (ARB), Surf. Coat. Technol. 361 (2019) 159–169. https://doi.org/10.1016/j.surfcoat.2019.01.043.
[9] L. Zhang, Z. Wang, Q. Li, J. Wu, G. Shi, et al., Microtopography and mechanical properties of vacuum hot pressing Al/B4C composites, Ceram. Int. 44 (2018) 3048–55. https://doi.org/10.1016/j.ceramint.2017.11.065.
[10] D.B. Miracle, S.L. Donaldson, S.D. Henry, C. Moosbrugger, G.J. Anton, et al., ASM Handbook, ASM International Materials Park, Ohio. 21 (2001).
[11] J. Hashim, L. Looney, M. Hashmi, Metal matrix composites: production by the stir casting method, J. Mater. Process. Technol. 92 (1999) 1–7. https://doi.org/10.1016/S0924-0136(99)00118-1.
[12] G. De With, Note on the temperature dependence of the hardness of boron carbide, J. Less-Common Met. 95 (1983) 133–138. https://doi.org/10.1016/0022-5088(83)90392-2.
[13] L. Zhang, J. Shi, Ch. Shen, X. Zhou, Sh. Peng, X. Long, B4C-Al composites fabricated by the powder metallurgy process, Appl. Sci. 7 (2017) 1009. https://doi.org/10.3390/app7101009.
[14] J. Onoro, M.D. Salvador, L.E.G. Cambronero, High-temperature mechanical properties of aluminium alloys reinforced with boron carbide particles, Mater. Sci. Eng. A. 499 (2009) 421–426. https://doi.org/10.1016/j.msea.2008.09.013.
[15] F. Toptan, A. Kilicarslan, A. Karaaslan, M. Cigdem, I. Kerti, Processing and microstructural characterisation of AA 1070 and AA 6063 matrix B4Cp reinforced composites, Mater. Des. 31 (2010) S87–S91. https://doi.org/10.1016/j.matdes.2009.11.064.
[16] M. Kubota, Solid-state reaction in mechanically milled and spark plasma sintered Al–B4C composite materials, J. Alloys Compd. 504 (2010) S319–S322. https://doi.org/10.1016/j.jallcom.2010.03.224.
[17] S. Chand, P. Chandrasekhar, R.K. Sarangi, R.K Nayak, Influence of B4C particles on processing and strengthening mechanisms in aluminum metal matrix composites-a review, Mater. Today Proc. 18 (2019) 5356–5363. https://doi.org/10.1016/j.matpr.2019.07.562.
[18] M. Li, K. Ma, L. Jiang, H. Yang, E. J Lavernia, et al., Synthesis and mechanical behavior of nanostructured Al 5083/n-TiB2 metal matrix composites, Mater. Sci. Eng. A. 656 (2016) 241–248. https://doi.org/10.1016/j.msea.2016.01.031.
[19] R. Casati, M. Vedani, Metal matrix composites reinforced by nano-particles—a review, Metals. 4 (2014) 65–83. https://doi.org/10.3390/met4010065.
[20] J. Abenojar, F. Velasco, M.A. Martinez, Optimization of processing parameters for the Al+ 10% B4C system obtained by mechanical alloying, J. Mater. Process. Technol. 184 (2007) 441–446. https://doi.org/10.1016/j.jmatprotec.2006.11.122.
[21] S. Jianmin, Z. Ling, C. Jing, S. Chunlei, L. Jiarong, Z. Xiaosong, Corrosion Behavior of Al-B4C Composite in Spent Nuclear Fuel Storage Environments, J. Chin. Soc. Corros. Prot. 33 (2013) 419–424.
[22] S.M.J. Mortazavi, M. Kardan, S. Sina, H. Baharvand, N. Sharafi, Design and fabrication of high density borated polyethylene nanocomposites as a neutron shield, Int. J. Radiat. Res. 14 (2016) 379.
[23] J. Lin, G. Ran, P. Lei, C. Ye, S. Huang, et al., Microstructure analysis of neutron absorber Al/B4C metal matrix composites, Metals. 7 (2017) 567. https://doi.org/10.3390/met7120567.
[24] P. Zhang, Y. Li, W. Wang, Z. Gao, B. Wang, The design, fabrication and properties of B4C/Al neutron absorbers, J. Nucl. Mater. 437 (2013) 350–358. https://doi.org/10.1016/j.jnucmat.2013.02.050.
[25] T. Yamazaki, K. Sanada, T. Nishiyama, H. Ishii, Development of neutron absorber (MaxusTm) for high burn-up spent nuclear fuel, Proceedings of the 15th International Symposium on the Packaging and Transportation of Radioactive Materials, Miami, Florida, USA. (2007) 1149–1154.
[26] X. Pang, Y. Xian, W. Wang, P. Zhang, Tensile properties and strengthening effects of 6061Al/12 wt% B4C composites reinforced with nano-Al2O3 particles, J. Alloys Compd. 768 (2018) 476–484. https://doi.org/10.1016/j.jallcom.2018.07.072.
[27] HS. Chen, WX. Wang, Y.L. Li, J. Zhou, H.H. Nie, Q.C. Wu, The design, microstructure and mechanical properties of B4C/6061Al neutron absorber composites fabricated by SPS, Mater. Des. 94 (2016) 360–367. https://doi.org/10.1016/j.matdes.2016.01.030.
[28] R. Belon, G. Antou, N. Pradeilles, A. Maître, D. Gosset, Mechanical behaviour at high temperature of spark plasma sintered boron carbide ceramics, Ceram. Int. 43 (2017) 6631–6635. https://doi.org/10.1016/j.ceramint.2017.02.053.
[29] D. Igwesi, O.S. Thomas, Determination of Thermal Neutron Macroscopic Cross Section for Two Polythene Based Slabs Using Monte Carlo N-Particle Code, J. Multidiscip. Eng. Sci. Technol. 1 (2014) 281–284.
[30] Standard Test Method for Water Absorption, Bulk Density, Apparent Porosity, and Apparent Specific Gravity of Fired Whiteware Products, ASTM C373-88(2006). https://doi.org/10.1520/C0373-88R06.
[31] D.B. Pelowitz, MCNPXTM user's manual, Los Alamos Natl. Lab. Los Alamos, USA. (2005).